Fabrication of selective injection microstructured optical fibers with a conventional fusion splicer

Limin Xiao, Wei Jin, M. S. Demokan, Hoi L. Ho, Yeuk L. Hoo, and Chunliu Zhao

Department of Electrical Engineering, The Hong Kong Polytechnic University, Kowloon, Hong Kong
xiaolimin.ee@polyu.edu.hk

Abstract: A simple method for fabricating selective injection microstructured optical fibers (MOFs) using a conventional fusion splicer is described. The effects of fusion current, fusion duration and offset position on the hole collapse property of the MOFs are investigated. With this method, the central hollow-core and the holes in the cladding region can be selectively infiltrated, which allows for the fabrication of novel hybrid polymer-silica and liquid-silica MOFs for various applications.

©2005 Optical Society of America

OCIS codes: (060.2310) Fiber optics; (230.3990) Microstructure devices

---

References and links

1. P. Domachuk, H.C. Nguyen, B.J. Eggleton, M. Straub, and M. Gu, "Microfluidic tunable photonic band-gap device," Appl. Phys. Lett. **84**, 1838-1840 (2004).
2. T.T. Larsen, A. Bjarklev, D.S. Hermann, and J. Broeng, "Optical devices based on liquid crystal photonic bandgap fibres," Opt. Express **11**, 2589-2596 (2003), http://www.opticsexpress.org/abstract.cfm?URI=OPEX-11-20-2589
3. C. Kerbage, R.S. Windeler, B.J. Eggleton, P. Mach, M. Dolinski, and J.A. Rogers, "Tunable devices based on dynamic positioning of micro-fluids in micro-structured optical fiber," Opt. Commun. **204**,179-184 (2002).
4. C. Kerbage, and B.J. Eggleton, "Numerical analysis and experimental design of tunable birefringence in microstructured optical fiber," Opt. Express **10**, 246-255 (2002), http://www.opticsexpress.org/abstract.cfm?URI=OPEX-10-5-246
5. C. Kerbage, P. Steinvurzel, P. Reyes, P. S. Westbrook, R. S. Windeler, A. Hale, and B. J. Eggleton, "Highly tunable birefringent microstructured optical fiber," Opt. Lett. **27**, 842-844 (2002).
6. F. Benabid, F. Couny, J.C. Knight, T.A. Birks, and P. St. J. Russell, "Compact, stable and efficient all-fibre gas cells using hollow-core photonic crystal fibres," Nature **434**, 488-491 (2005).
7. F. Benabid, G. Bouwmans, J.C. Knight, P. St. J. Russell, and F. Couny, "Ultrahigh efficiency laser wavelength conversion in a gas-filled hollow core photonic crystal fiber by pure stimulated rotational raman scattering in molecular hydrogen," Phys. Rev. Lett. **93**,123903 (2004).
8. T. M. Monro, W. Belardi, K. Furusawa, J. C. Baggett, N. G. R. Broderick, and D. J. Richardson, "Sensing with microstructured optical fibres," Meas. Sci. Technol. **12**, 854-858 (2001).
9. J. B. Jensen, L. H. Pedersen, P. E. Hoiby, L. B. Nielsen, T. P. Hansen, J. R. Folkenberg, J. Riishede, D. Noordegraaf, K. Nielsen, A. Carlsen, and A. Bjarklev, "Photonic crystal fiber based evanescent-wave sensor for detection of biomolecules in aqueous solutions," Opt. Lett. **29**, 1974-1976 (2004).
10. Y. L. Hoo, W. Jin, C. Shi, H. L. Ho, D. N. Wang, and S. C. Ruan, "Design and modeling of a photonic crystal fiber gas sensor," Appl. Opt. **42**, 3509-3515 (2003)
11. J. M. Fini, "Microstructure fibres for optical sensing in gases and liquids," Meas. Sci. Technol. **15**, 1120-1128 (2004).
12. Y. Huang, Y. Xu, and A.Yariv, "Fabrication of functional microstructured optical fibers through a selective-filling technique," Appl. Phys. Lett. **85**, 5182-5184 (2004).
13. C. Martelli, J. Canning, K. Lyytikainen, and N. Groothoff, "Water-core fresnel fiber," Opt. Express **13**, 3890-3895 (2005), http://www.opticsexpress.org/abstract.cfm?URI=OPEX-13-10-3890
14. S. Yiou, P. Delaye, A. Rouvie, J. Chinaud, R. Frey, G. Roosen, P. Viale, S. Février, P. Roy, J. Auguste, and J. Blondy, "Stimulated raman scattering in an ethanol core microstructured optical fiber," Opt. Express **13**, 4786-4791 (2005), http://www.opticsexpress.org/abstract.cfm?URI=OPEX-13-12-4786
15. K. Nielsen, D. Noordegraaf, T. Sørensen, A. Bjarklev, and T. P. Hansen, "Selective filling of photonic crystal fibres," J. Opt. A: Pure Appl. Opt. **7**, L13-L20 (2005).
16. B. Bourliaguet, C. Paré, F. Émond, A. Croteau, A. Proulx, and R. Vallée, "Microstructured fiber splicing," Opt. Express **11**, 3412-3417 (2003), http://www.opticsexpress.org/abstract.cfm?URI=OPEX-11-25-3412

17. A. D. Yablon, and R. T. Bise, "Low-loss high-strength microstructured fiber fusion splices using grin fiber lenses," IEEE Photonics Technol. Lett. **17**, 118-120 (2005).
18. M. Tachikura, "Fusion mass-splicing for optical fibers using electric discharges between two pairs of electrodes," Appl. Opt. **23**, 492-498 (1984).
19. A. D. Yablon, *Optical fiber fusion splicing*, (Heidelberg, Germany: Springer-Verlag press, 2005).
20. *User's manual for the FSU 975 single fiber fusion splicer by Ericsson.*

_____

1. Introduction

Microstructured optical fibers (MOFs) with their holes filled with gas or liquid have been actively studied for a number of years. The applications of these fibers include tunable fiber optic devices [1-5], laser sources [6, 7] and waveguide sensors [8-11]. Most of the MOF sensors studied previously have solid cores and exploit the interaction of light with samples through evanescent field extended into the air holes [8-10]. The air holes also act as channels to confine gas or liquid samples. The advantages of MOF sensors, compared with other evanescent wave sensors, include long interaction length which improves the sensitivity, and the robust structure without needing to remove the fiber cladding and polymer coating [9]. However, evanescent-field sensors have poor light field/sample overlap and hence relatively low sensitivity. Recently, it has been reported that hollow-core MOFs have been used for sensing in gas and liquid [11]. In liquid sensing, the core is formed by a liquid sample and is surrounded by an air-silica microstructured cladding; the filling of liquid into the core turns the photonic bandgap guidance into total internal reflection guidance [11]. This novel design has many key advantages over evanescent-field sensors: near-unity light/sample overlap over a wide range of wavelength range, and a single mode or a few low-order modes can be propagated in the liquid core if the average air-silica cladding index is just below the index of the liquid. This novel structure not only introduces an effective way for liquid sensing applications, but also opens new perspectives for nonlinear applications by filling various functional materials into the central hole of a MOF.

In practical realization, however, filling only the central core of a MOF but not the others is a major challenge [11, 12]. To our knowledge, only a few articles [4, 5, 13-15] reported works on the selective filling of the holes in a MOF. In [4, 5], selective filling of six-hole microstructured fiber to achieve tunable birefringence is described. In [12], the authors fill the central hollow core by differential filling speed that depends on the size of the air holes; the fabrication process is very complicated because a UV curable polymer and a multi-step injection-cure-cleave process are needed. In [13], a single-hole hollow-core fiber is spliced to the MOF using a fusion splicer; the single-hole is aligned to the central hole of the MOF and cladding holes are sealed by the solid cladding of the single-hole fiber. In this method, a hollow fiber with a suitable single-hole size is needed and the silica bridge between the central hole and cladding holes of the MOF can't be too thin, which limits this method for widespread applications. In [14, 15], the authors mention briefly the use of a fusion splicer to collapse the cladding holes for the fabrication of liquid core MOF but don't give details on the fusion process and how the fusion parameters affect the results. In this paper, we report a simple method for selective filling of the central hole. The method uses only a conventional fusion splicer, and by proper selection of fusion parameters, the cladding holes can be closed while the central hole remains open. The effects of fusion current, fusion duration and offset position on the hole collapse property of the MOFs are investigated.
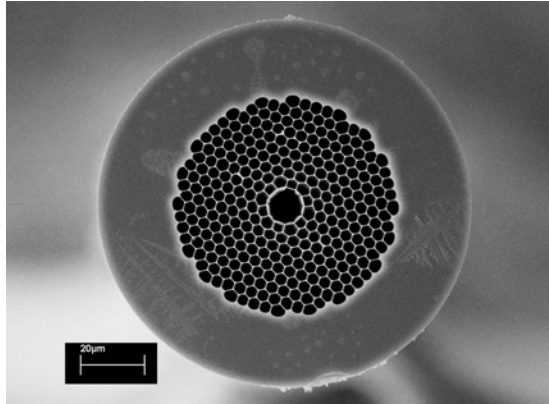
2. Method of fabrication

Fig. 1. SEM image of the cross section of the MOF used for the experiment.

Figure 1 shows a Scanning Electron Microscope (SEM) micrograph of the MOF cross-section. The MOF was purchased from Crystal-Fiber A/S and has a central hole of diameter 10.9µm. The central hole is surrounded by a holey lattice of pitch 3.8µm. The holey cladding region has a diameter of 70µm and is surrounded by a ring of solid silica. The total diameter of the fiber is about 120µm. The thickness of the silica layers between cladding holes is about 0.36µm, and the air-filling fraction in the holey region is above 90%. This fiber is a good candidate for fabricating a novel liquid-core MOF as discussed in [11] because the average index of air-silica cladding is sufficiently low to allow the guidance of light in almost any liquid-core through total internal reflection.

In the following, we discuss the use of a conventional fusion splicer to selectively collapse some or all of the holes in the cladding but leave the central-hole remain open. The conventional fusion splicer has been used to splice a MOF to a standard single mode fiber (SMF). In such an operation, an effective approach to achieve low splicing loss is to use an arc of short duration and weak discharge current to avoid or reduce the collapse of the holes of the MOF[16, 17]. In standard fiber splicing, the electrode axis is positioned at the center-line as shown in Fig. 2(a), and the ends of the two fibers are affected equally by the discharge. Since the holes in the end part of a MOF are easy to collapse, if the electrode axis is positioned as shown in Fig. 2(b), the arc discharge will affect the end face of a MOF only weakly as compared with the end-face of the solid SMF. We define the "offset" as the distance between the tip of the MOF and the electrode axis. Such an arrangement avoids the total collapse of the cladding holes and hence reduces the splicing loss. We propose in this paper to use the offset to selectively control the collapse of the holes at the end-face of a MOF. By removing the standard SMF just before the start of the arc discharge, the end face of the MOF will not be spliced to the SMF and it will only be heated by a weak arc discharge that will cause the collapse of some of the holes.
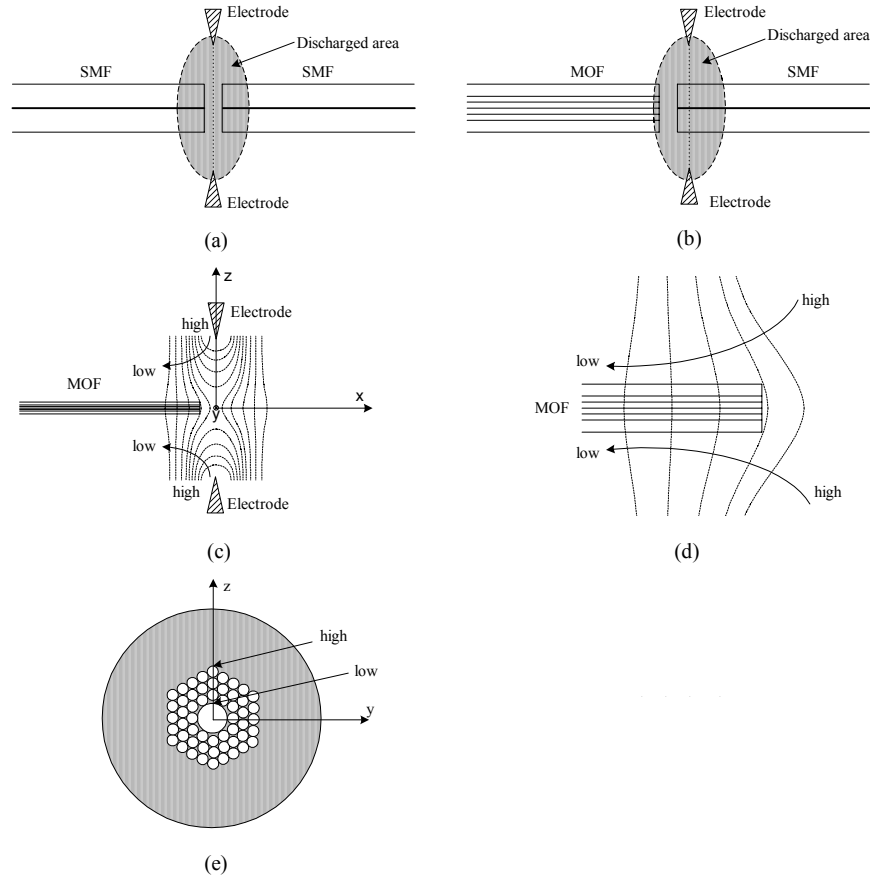
Fig. 2. The positioning of the electrode axis when (a) two SMFs are to be fusion spliced, (b) a SMF is to be spliced to a MOF, (c) The current and energy density distribution in an arc fusion splicer[18,19], (d) The close-up of the end part of the MOF in the temperature(energy density) distribution field of Fig. 2(c), (e) Illustration of the transverse temperature distribution in the MOF.

The current density between two electrodes is given by [18, 19]

$$i(r,z) = \frac{I_0}{2\pi\sigma^2(z)}\exp(-\frac{r^2}{2\sigma^2(z)}),$$ (1)

where

$$\sigma(z) = \sigma_0(1+Cz^2)^{-1/3}, \quad r^2 = x^2 + y^2.$$ (2)

The coordinates x, y and z are defined in Fig. 2(c). I_0 is the total current that can be obtained by integrating the current density over all r. $\sigma(z)$ is the Gaussian width of the current density at position z, σ_0 is the Gaussian width of the current density at the midpoint of the electrodes' separation (z=0), C is a constant determined from the variation of the square of the current density in the z direction. Figure 2(c) shows the current density or energy density distribution by contour lines, Fig. 2(d) is the close-up of the end part of the MOF in the temperature (energy density) distribution field in Fig. 2(c). The energy density changes with the square of the current density and the temperature of the discharge is proportional to the energy density [18, 19]. From Eqs. (1) and (2), we can find the arc discharge is hottest at the electrode tips

and the temperature at the midpoint between the electrode tips falls to a minimum along the electrode's axis, hence the temperature distribution of the end face of MOF is that the inner cladding temperature is lower than the outer cladding temperature (Figs. 2(d) and 2(e)) when the tip of the MOF is not too far from the electrode axis, i.e. when the offset is small. For a standard SMF, the fiber temperature is largely uniform along the fiber radial direction because the thermal conduction time of the solid SMF is very short, only a few milliseconds are required to transfer heat from the hottest spot of the outer surface to the center and other locations within the fiber cross-section and to establish a uniform temperature distribution across the whole cross-section [19]. For the solid silica ring cladding of the MOF, the condition is similar to the solid SMF, so the temperature of the solid ring cladding can be regarded as uniform. However, the heat transfer from the solid silica ring to the center of the holey region is much slower because of the presence of large air-holes and the relative slow heat transfer in air than in solid silica. Hence it is believed that temperature of the inner cladding holes will keep lower than that of the outer cladding holes during the discharge duration which is typically a few hundreds milliseconds. It is difficult to accurately determine the temperature distribution around the holly region. However, from the data of [18], the temperature decreases by about 200 ^{o}C from the point z=500 μm to the midpoint along the electrode's axis, we may qualitatively estimate the temperature difference between the outer cladding holes and the inner cladding holes at about (200°C /500μm)*35μm =14 ^{o}C. The temperature decreases as a Gaussian function when the offset from the electrode axis increases. From [18], we also know that when the offset is changed by 100 μm under the same fusion current and fusion duration, the temperature changes by about 100°C.

When the temperature of heated fiber exceeds the softening point which is around 1670°C, the surface tension will overcome the viscosity and cause the MOF's cylindrical air holes to begin collapsing. The rate of collapse is given by [17,19]

$$V_{collapse} = \frac{\gamma}{2\eta} \qquad (3)$$

where γ is surface tension and η is viscosity. Surface tension of silica is not very sensitive to temperature over the range encountered in splicing; but in contrast, the viscosity of silica decreases sharply with increasing temperature, so the air holes collapse quickly in the high temperature region. Since the temperature at the center of the MOF will be lower as compared to the periphery and also since the smaller hole will close before the bigger hole, the air holes in the cladding will close before the central hole. The combined effect of temperature distribution and hole-size allows for the fabrication of selective injection MOFs by using arc discharge of a conventional fusion splicer.

3. Experiments and results

We investigated experimentally the effects of fusion parameters on the collapse of holes of the MOF shown in Fig. 1. An Ericsson FSU-975 fusion splicer was used in the experiments. The typical parameters-set for splicing two SMFs are: gap 50μm, overlap 10 μm, prefusion time 0.2s, prefusion current 10.0mA; fusion time one 0.3s, fusion current one 10.5mA; fusion time two 2.0s, fusion current two 16.3mA; fusion time three 2.0s, fusion current three 12.5mA; the center position is 255. During prefusion the fibers are cleared by low level heating, and the main fusion process is fusion time two [20]. Hence we set the fusion time one and three to zero and varied fusion time two and fusion current two to perform discharge tests and the end-face image of the MOF was taken by a scanning electron microscope. The prefusion current was set to 8.0mA instead of 10mA to avoid heat collapse of the holes at the MOF end face. We firstly set the center position to 205 which means the offset distance is 50μm, and set the overlap to 0 μm to get a precise offset distance of the MOF end-face that was subject to heating by arc discharge; we then varied the fusion time, fusion current, and fusion center position to see the effect of these parameters on the collapse of cladding and central holes. Optimal parameters that correspond to the collapse of the cladding holes with the central hole

remaining open were then found and used to fabricate the selective injection of a MOF.

3.1 The effect of fusion current

We varied the fusion current in steps of 0.5mA, kept the fusion duration constant at 0.3s, and offset distance constant at 50μm. Fig. 3(b, c) shows the end-face of the MOF for two typical discharge conditions. The surface tension makes the MOF's periphery less sharp and causes the central region to cave in. The detailed hole collapse pictures can be found in Fig.4.
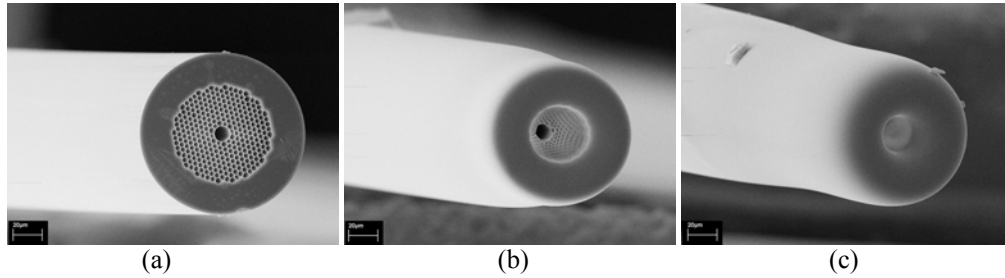

| (a) | (b) | (c) |

Fig. 3. End-face of the MOF. (a) without arc discharge; (b) arc current =12.5mA; (c) arc current =14.5mA. The discharge duration and offset distance are kept constant at 0.3 second and 50 μm, respectively.

It can be seen from Fig. 4, when arc current is increased, the outer cladding holes collapse and close first when compared to the inner cladding holes.
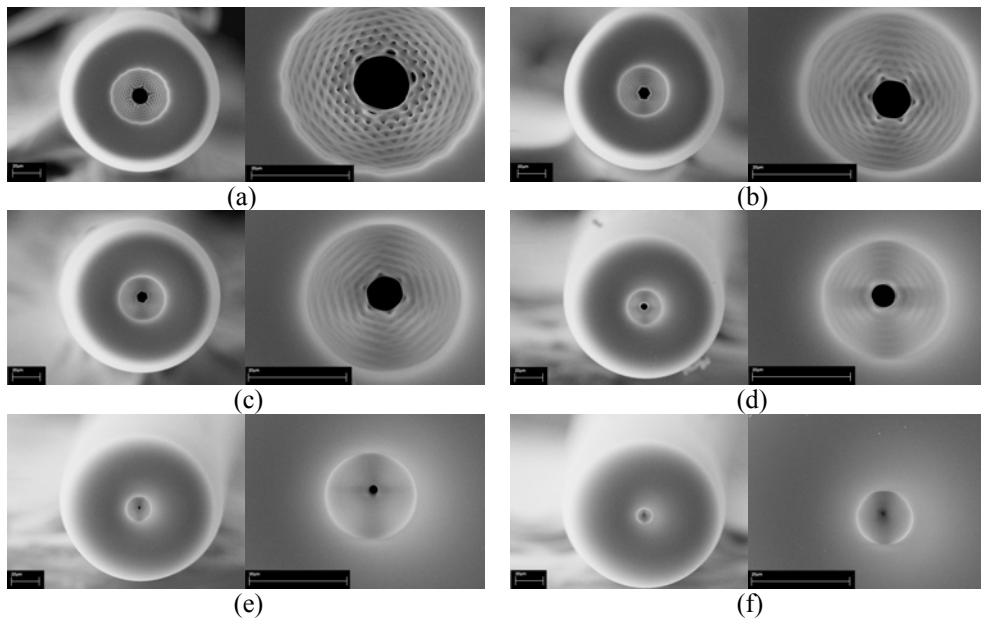

Fig. 4. End views of the MOF with different arc currents when the arc duration is 0.3 second and the offset distance is 50μm. The right picture is the close-up of the center part of the left picture. (a) 12.5mA, (b) 13mA, (c) 13.5mA, (d) 14mA, (e) 14.5mA, (f) 15mA.

At 12.5mA, the outer-most holes have already closed but the inner holes are still partially open, as shown in Fig. 4(a). From the close-up picture in Fig. 4(a), we can find the gradual change of the hole size along the radical direction of the fiber. The nearer the holes to the center, the less complete will be the holes' collapse. As hole-sizes of the inner and outer claddings are more or less the same (as shown in Fig. 1), we believe that the variation in hole collapse along the fiber radical direction is due to a gradual decrease of temperature from the

outer solid ring to the central hole. Increasing the temperature by increasing the fusion current enables more holes to collapse within the fusion duration, eventually all the holes in the cladding region close and the central hole can be kept partially open due to the combined effect of lower temperature at and the larger hole size of the central hole. If we continue to increase fusion current, the central hole will shrink and eventually also close. At 13mA, almost all the cladding holes have closed except the inner six holes that are nearest to the central hollow-core (Fig. 4(b)). From Fig.1, we can see that these six holes, due to fabrication imperfection, have slightly bigger sizes than the other six holes surrounding the central-hole. At 13.5mA (Fig. 4(c)), all the holes in the cladding region are closed, although the edge of the central hole is not very smooth. The diameter of the central hole has reduced to about 7.2μm. When the fusion current reaches 14.0mA, the collapsed region is very smooth and the central hole's diameter shrinks to about 4.7μm, as can be seen from Fig. 4(d). The diameter of the central hole decreases further at 14.5mA and finally the hole closes totally (Fig. 4(f)) when the current is beyond 15mA. The experimental observation agrees with the discussion in section 2.

3.2 The effect of fusion duration

We also evaluated the effect of varying the duration of the arc current when the fusion current and offset distance were kept constant. Figure 5 shows the results for arc current of 13.5mA and offset distance of 50μm when the arc duration is varied from 0.3 second to 0.5 second. The central hole shrunk from 7.2μm to about 4.0μm when the arc duration was increased from 0.3s to 0.4s, and further reduced to about 2.5μm when the arc duration increased to 0.5s. Further increase the arc duration closed all the holes in the center and the cladding. From the discussion in section 2, the outer solid ring cladding will transfer heat to the holey cladding in the fiber radial direction. With the fusion duration increasing, more heat can be transferred to the central hole and the temperature of the central hole increases, so the central hole's size decreases when the fusion duration increases.
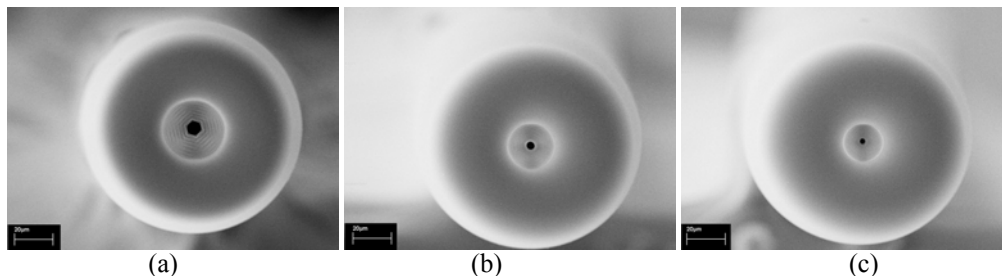

(a) (b) (c)

Fig. 5. End views of the MOF with different arc durations. (a) 0.3 second, (b) 0.4 second, and (c) 0.5 second. The arc current and offset distance are kept constant at 13.5mA and 50μm, respectively.

3.3 The effect of fusion offset

Figure 6 shows the SEM micrographs of the MOF end-face for various offset distances, varying from 50μm to 0 (no offset). For the cases shown in Fig. 6, all the holes in the cladding are closed, and the size of the central hole reduces for smaller offset distance and closes for zero offset. This is because that temperature around the end-face is higher for smaller offset. From the discussion in section 2, the temperature increases by about 10 $^{\circ}$C when the offset decreases by 10μm, so the central hole collapses more quickly in the higher temperature caused by smaller offset.
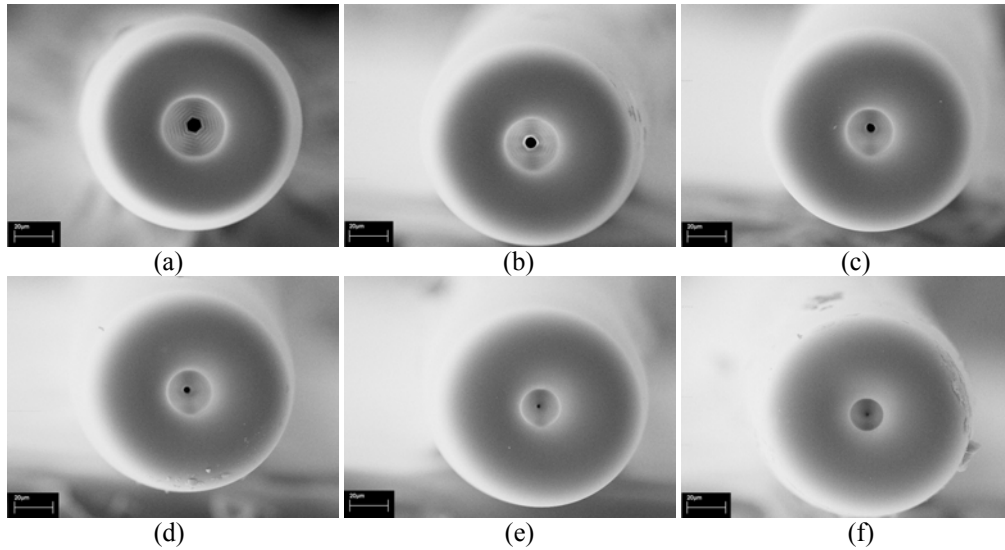
Fig. 6. End views of the MOF with different offset distances when the arc duration and arc current are fixed at 0.3 second and 13.5mA, respectively. (a) 50μm, (b) 40μm, (c) 30μm, (d) 20μm, (e) 10μm, (f) 0μm.

3.4 Filling the central hole of MOF

To demonstrate the above technique can be used to perform selective filling of the central hole, we used about 15cm of MOF with cross-section similar to that shown in Fig. 1. We firstly treated the two ends of the MOF with an Ericsson FSU-975 fusion splicer with arc duration, fusion current and offset distance set respectively to 0.3 second, 14mA and 50μm. After thermal treatment, both ends of the MOF were like Fig. 4(d), that is, the central hole is still partially open, and all the cladding holes are totally closed. The central hole was then filled with a type of polymer NOA74 by capillary action, the polymer was cured by a UV lamp and the ends of the MOF were cleaved. The two cleaved ends were then examined by using an optical microscope and a scanning electron microscope. The images of one of the ends are shown in Fig. (7). The central hole is perfectly filled and the holes in the cladding are not filled. We have thus demonstrated how the hollow core of a MOF can be filled with liquid or gas without filling the cladding holes at the same time. The same results have been obtained with other fusion conditions as given in Fig. 4(c) and Fig. 4(e). This demonstrates the effectiveness of the method for fabricating selective injection MOFs.
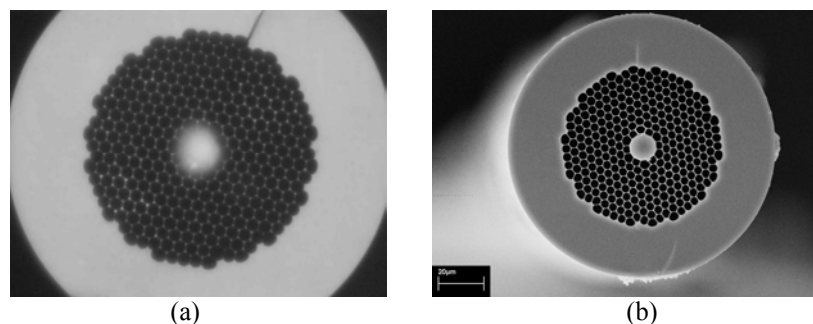

Fig. 7. (a) Optical microscope image and (b) SEM image of the MOF with the central hole filled with NOA74.

4. Conclusion

In conclusion, we have developed a simple method for selective filling the central hole of MOFs. The method is based on a conventional fusion splicer to cause the cladding holes to collapse while leaving the central hollow core to remain open. Theoretical and experimental investigations show that the hole-collapse property of a MOF depends on fusion current, fusion duration and fusion offset position. The opening and closing of the central hole and the holes in the cladding may be controlled to a certain degree by controlling the fusion current, the fusion duration and the fusion offset position. Experiments show that this method can be used to make hybrid polymer/silica MOFs with the central hole filled by a polymer. The quality of the hybrid fiber is good and the fabrication process is highly reproducible. The authors believe that this method can also be used in other MOFs with different structures by adjusting the fusion parameters. This method can also be used to fabricate a hybrid MOF with a liquid or gas core surrounded by an air-silica microstructured cladding.